Tanshinone IIA Attenuates Atherosclerosis in Apolipoprotein E Knockout Mice Infected with Porphyromonas gingivalis

Yan Xuan, Yue Gao, Hao Huang, Xiaoxuan Wang, Yu Cai & Qing Xian Luan

Volume 40, Number 5

October 2017

40(5) 1475–1814 (2017)
ISSN 0360-3997

Inflammation

Springer

Springer

Springer

CrossMark

ORIGINAL ARTICLE

Tanshinone IIA Attenuates Atherosclerosis in Apolipoprotein E Knockout Mice Infected with *Porphyromonas gingivalis*

Yan Xuan,[1,2] Yue Gao,[3] Hao Huang,[3] Xiaoxuan Wang,[1] Yu Cai,[1,2,4,5] and Qing Xian Luan[1,4,5]

Abstract—Tanshinone IIA (TSA), a pharmacologically active component isolated from Danshen, may prevent cardiovascular diseases due to its anti-inflammatory, anti-oxidative, and anti-adipogenic effects. *Porphyromonas gingivalis*, a major periodontal pathogen, may contribute to the progression of atherosclerosis. Here, we studied the effects of TSA on atherosclerosis in ApoE$^{-/-}$ mice with *P. gingivalis* infection. Eight-week-old ApoE$^{-/-}$ mice were randomized to (a) phosphate-buffered saline (PBS), (b) *P. gingivalis*, and (c) *P. gingivalis* + TSA (60 mg kg^{-1} day^{-1}). The mice were injected with (a) PBS, or (b) and (c) *P. gingivalis* 3 times per week for a total of 10 times. After 8 weeks, atherosclerotic risk factors in serum and in heart, aorta, and liver tissues were analyzed in all mice using Oil Red O, atherosclerosis cytokine antibody arrays, enzyme-linked immunosorbent assay (ELISA), real-time PCR, and microRNA array. CD40, G-CSF, IFN-γ, interleukin (IL)-1β, IL-6, MCP-1, MIP-3α, tumor necrosis factor-α (TNF-α), and VEGF were attenuated by TSA in atherosclerosis cytokine antibody arrays. TSA-treated mice showed a significant reduction of C-reactive protein (CRP), ox-LDL, IL-1β, IL-6, IL-12, and TNF-α in ELISA data. Real-time PCR analyses showed that TSA decreased the expression of CCL-2, CD40, IL-1β, IL-6, TNF-α, and MMP-2 in heart and aorta tissues. Moreover, hepatic CRP was downregulated by TSA, although FASN and HMG-CoA were not. The relative expressions of miR-146b and miR-155 were elevated by *P. gingivalis* infection and were downregulated by TSA treatment.

QingXian Luan and Yu Cai contributed equally.

[1] Department of Periodontology, Peking University School and Hospital of Stomatology, National Engineering Laboratory for Digital and Material Technology of Stomatology, Beijing Key Laboratory of Digital Stomatology, 22 Zhongguancun Avenue South, Haidian District, Beijing, 100081, China

[2] Central Laboratory, Peking University School and Hospital of Stomatology, National Engineering Laboratory for Digital and Material Technology of Stomatology, Beijing Key Laboratory of Digital Stomatology, 22 Zhongguancun Avenue South, Haidian District, Beijing, 100081, China

[3] Department of Pharmacology and Toxicology, Institute of Radiation Medicine, Academy of Military Medical Sciences, Beijing, China

[4] National Engineering Laboratory for Digital and Material Technology of Stomatology, Beijing Key Laboratory of Digital Stomatology, Peking University School and Hospital of Stomatology, 22 Zhongguancun Avenue South, Haidian District, Beijing, 100081, People's Republic of China

[5] To whom correspondence should be addressed at National Engineering Laboratory for Digital and Material Technology of Stomatology, Beijing Key Laboratory of Digital Stomatology, Peking University School and Hospital of Stomatology, 22 Zhongguancun Avenue South, Haidian District, Beijing, 100081, People's Republic of China. E-mails: jessonjesson@hotmail.com; kqluanqingxian@163.com

Abbreviations: TSA, Tanshinone IIA; *P. gingivalis*, *Porphyromonas gingivalis*; ApoE $^{-/-}$ mice, Apolipoprotein E knockout mice; AS, Atherosclerosis; PBS, Phosphate-buffered saline; GAPDH, Glyceraldehydes 3-phosphate dehydrogenase; bFGF, Basic fibroblast growth factor; IL-1β, Interleukin-1β; TNF-α, Tumor necrosis factor-α; IFN-γ, Interferon-γ; VEGF, Vascular endothelial growth factor; G-CSF, Granulocyte-colony stimulating factor; MCP-1, Monocyte chemoattractant protein-1; MIP-3α, Macrophage inflammatory protein-3α; CRP, C-reactive protein; IL-6, Interleukin-6; IL-12, Interleukin-12; ox-LDL, Oxidized low-density lipoprotein; HDL, High-density lipoprotein; LDL, Low-density lipoprotein; VLDL, Very low-density lipoprotein; MMP-2, Matrix metallopeptidase-2; MMP-9, Matrix metallopeptidase-9; LOX-1, Lectin-like ox-LDL receptor-1; COX-2, Cyclooxygenase-2; FASN, Fatty acid synthase; HMG-COA, 3-hydroxy-3-methylglutaryl coenzyme A; MI, Myocardial infarction; ICAM-1, Intercellular cell adhesion molecule-1; HUVECs, Human umbilical vein endothelial cells; LPS, Lipopolysaccharide

These results suggest that TSA was a potential therapeutic agent that may have the ability to prevent *P. gingivalis*-induced atherosclerosis associated with anti-inflammatory and anti-oxidative effects.

KEY WORDS: atherosclerosis; *Porphyromonas gingivalis*; tanshinone IIA; ApoE$^{-/-}$ mice; anti-inflammatory; anti-oxidative.

INTRODUCTION

Atherosclerosis is a multifactorial cardiovascular disease and is one of the most prevalent fatal diseases in the world. It is characterized by initial lipid deposition and inflammatory response in the intima. Inflammation and oxidative stress are considered to play pivotal roles in the development of atherosclerosis and formation of plaques [1]. Periodontitis is a chronic inflammatory disease resulting in the destruction of tooth-supporting tissues, including the resorption of alveolar bone and the periodontal ligament, eventually leading to tooth loss. Periodontitis is associated with systemic diseases such as cardiovascular disease, diabetes, and osteoporosis [2–4]. Furthermore, epidemiological studies have revealed that periodontitis is closely associated with atherosclerosis, and periodontal pathogens are positively associated with the incidence of cardiovascular diseases [5].

Porphyromonas gingivalis (*P. gingivalis*) is a Gram-negative, non-motile, anaerobic bacterium. It is not only one of the most important pathogens associated with chronic periodontitis but also is an important risk factor for atherosclerosis [6–10]. *P. gingivalis* infection can increase inflammatory markers; the pathogen invades vascular smooth muscle cells and endothelial cells to accelerate the progression of atherosclerosis [11, 12]. Previous studies have indicated that *P. gingivalis* infection can activate inflammatory mediators in response to *P. gingivalis*-accelerated atherosclerosis [13].

Tanshinone IIA (TSA) is a major bioactive lipophilic constituent isolated from Danshen, which is the root of the herb *Salvia miltiorrhiza* Bunge used in traditional Chinese medicine (Fig. 1). TSA was found to have cardioprotective and anti-atherosclerotic effects [14] due to its anti-oxidative [15], anti-inflammatory [16], and anti-adipogenic [17] effects. TSA has an anti-oxidative effect and prevents atherosclerosis by reducing vascular oxidative stress, inhibiting platelet aggregation, and protecting from endothelium damage [18]. Anti-inflammatory and immunomodulatory effects of TSA for atherosclerosis have been recently highlighted [16].

Therefore, the aim of this study was to examine whether TSA attenuates the development of atherosclerosis induced by *P. gingivalis* in apolipoprotein E knockout (ApoE$^{-/-}$) mice, and to observe the expression of factors associated with atherosclerosis in the serum and in heart, aorta, and liver tissues, in order to assess the possible anti-inflammatory and anti-oxidative effects of TSA. Due to the ApoE$^{-/-}$ congenital defect affecting lipid metabolism, the ApoE$^{-/-}$ mice are at greater risk of developing atherosclerosis under certain conditions (*e.g.* pathogen infection), independently of diet [8, 10, 19]. Since a high-fat diet can induce atherosclerosis by itself, a normal diet was used in these mice to avoid the confounding factor.

MATERIALS AND METHODS

Bacterial Culture

The *P. gingivalis* strain FDC381 was cultured under anaerobic conditions (80% N_2, 10% CO_2, and 10% H_2) on 5% sheep blood anaerobic basal agar plates (Oxoid Ltd., England) at 37 °C for 3–5 days. Cultures were inoculated into a brain heart infusion broth (Oxoid Ltd., England) with 5 μg mL^{-1} hemin and 0.4 μg mL^{-1} menadione (Sigma-
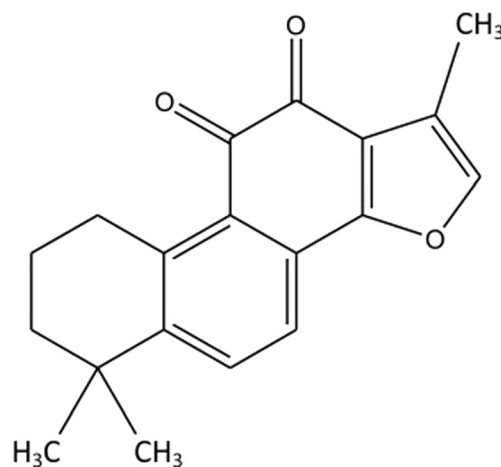

Fig. 1. Structure of tanshinone IIA (TSA).

Aldrich, USA), and grown for 2 days at 37 °C until they reached an optical density at 600 nm (OD_{600}) of 1.0, corresponding to 10^9 CFU mL^{-1}. Bacterial suspensions were centrifuged at 8000×g for 20 min at 4 °C and diluted with phosphate-buffered saline (PBS) for intravenous injection.

Mice and Treatments

Six-week-old male ApoE$^{-/-}$ mice (C57BL/6) were purchased from Vital River, Inc. (Beijing, China) and housed under specific pathogen-free conditions. They were fed sterile food and distilled water *ad libitum*. The Institutional Animal Care and Use Committee of Peking University Health Science Center approved the present study and experiments (approval number LA201464). After 2 weeks of housing, the mice were divided randomly into three groups ($n = 8$/group): (a) ApoE$^{-/-}$ + PBS, (b) ApoE$^{-/-}$ + *P. gingivalis*, and (c) ApoE$^{-/-}$ + *P. gingivalis* + TSA. The mice were inoculated intravenously 10 times, three times/ week, with (a) PBS (100 μL per mouse) or (b) and (c) *P. gingivalis* (10^8 CFU 100 μL^{-1} per mouse). For group (c), TSA (Sigma-Aldrich, USA) was dissolved in 0.5% carboxymethylcellulose (CMC; Sigma-Aldrich, USA) for oral gavage at a dose of 60 mg kg^{-1} bw day^{-1}, as described previously [20]. At the age of 16 weeks, the mice were sacrificed to collect blood and tissue samples.

Tissue Preparation

Mice continued to receive normal food and distilled water with or without TSA until 16 weeks of age. All mice were euthanized by intraperitoneal pentobarbital sodium (100 μg μL^{-1}, Merck, Germany). Blood samples were collected by infraorbital puncture, and serum was isolated by centrifugation at 10,000 rpm for 5 min at 4 °C. The heart and aorta were perfused through the left ventricle with heparinized ice-cold 0.9% PBS for 10 min. The components of the heart (including the aortic root) were carefully dissected, embedded with OCT compound (Tissue-Tek, Torrance, CA, USA), and frozen for cryosections. The liver was rapidly removed from the mice, placed in liquid N_2, and kept at −80 °C.

Oil Red O Staining

Cryosections of the aortic sinus were prepared for Oil Red O staining. Atherosclerotic lesions were measured following the modified method of Paigen *et al.* [21]. Each section was captured by optical microscopy (Nikon Eclipse-Ci, Japan) and a digital camera (Olympus Q-

Color 5, Japan). Total lesion area and percentage of the aortic lumen occupied by lesions per section (5-μm thickness) were calculated using the Image-Pro Plus software 6.0 (Media Cybernetics, USA). The values of 15 sections per animal were averaged and expressed as percentage of the lumen of the proximal aorta occupied by lesions per section per animal.

Antibody Array

The serum samples were analyzed using the Mouse Atherosclerosis Antibody Array C1 (RayBiotech, USA), which consists of 22 different atherosclerosis-related cytokine antibodies, following the manufacturer's recommendations and as previously described [6]. The signal intensities of spots were measured using a Vilber Lourmat Fusion-FX system (Marne-la-Vallée Cedex, France) and analyzed using the mouse atherosclerosis cytokine semiquantitative software. Six positive control spots were used to identify the membrane orientation and to normalize the results from different membranes (Table 1). The net optical density level of each spot was determined by subtracting the background optical level from total raw optical density, and the level of each cytokine was represented as a percentage of the positive control. The list of the cytokines examined is shown in Table 1.

Cytokine ELISA

Serum samples were isolated from blood after euthanasia. Commercial enzyme-linked immunosorbent assay (ELISA) kits were used to quantify the serum levels of interleukin-1β (IL-1β), interleukin-6 (IL-6), and tumor necrosis factor-α (TNF-α) (RayBiotech, USA); interleukin-12 (IL-12) (eBioscience, USA); and C-reactive protein (CRP) (TSZ Biosciences, USA). ELISA kits were also used to quantify oxidized low-density lipoprotein (ox-LDL) (Cusabio, China), high-density lipoprotein (HDL) (TSZ Biosciences, USA), and low-density lipoprotein (LDL)/very low-density lipoprotein (VLDL) (TSZ Biosciences, USA).

Quantitative Real-Time PCR

Total RNA was purified from heart, aorta, and liver tissues using the RNeasy Fibrous Tissue Kit (Qiagen, USA) and RNeasy Plus Mini Kit (Qiagen, USA). Following reverse transcription using the PrimeScript RT Master Mix kit (Takara Bio, Japan) to generate complementary DNA (cDNA), quantitative real-time polymerase chain reaction (PCR) analysis was performed using an Applied

Table 1. Mouse Atherosclerosis Antibody Array Map

	A	B	C	D	E	F	G	H
1	POS	POS	NEG	NEG	BLANK	bFGF	CD40	Eotaxin-1
2	POS	POS	NEG	NEG	BLANK	bFGF	CD40	Eotaxin-1
3	G-CSF	GM-CSF	IFN-γ	IL-1α	IL-1β	IL-2	IL-3	IL-4
4	G-CSF	GM-CSF	IFN-γ	IL-1α	IL-1β	IL-2	IL-3	IL-4
5	IL-5	IL-6	IL-13	L-selectin	MCP-1	M-CSF	MIP-3α	P-selectin
6	IL-5	IL-6	IL-13	L-selectin	MCP-1	M-CSF	MIP-3α	P-selectin
7	RANTES	TNF-α	VEGF	BLANK	BLANK	BLANK	BLANK	POS
8	RANTES	TNF-α	VEGF	BLANK	BLANK	BLANK	BLANK	POS

POS positive control spot, *NEG* negative control spot, *BLANK* blank

Biosystems 7500 Fast Real-Time PCR System (Life Technologies, USA) in accordance with the manufacturer's protocol. Briefly, the reactions contained 10 μL of 2× SYBR Green (Takara Bio, Japan), 100 nM of each primer, and 30 ng of reverse-transcribed RNA. The PCR conditions were 95 °C for 30 s, followed by 40 cycles at 95 °C for 5 s and 60 °C for 34 s. Dissociation curve analysis was performed to confirm specificity. Each gene was tested in triplicate, and target RNA levels were normalized to glyceraldehyde 3-phosphate dehydrogenase (GAPDH) messenger RNA (mRNA). Primer sequences are shown in Table 2.

MicroRNA Array and Quantitative Real-Time PCR

MicroRNA (miRNA) fractions from the hearts of the mice were isolated using the miRcute miRNA Isolation Kit (Tiangen, China), according to the manufacturer's instructions. miRNA were reverse transcribed using the miRcute miRNA cDNA First-Strand cDNA Synthesis Kit (Tiangen,

China). The miRcute miRNA qPCR Detection Kit (SYBR Green, Tiangen, China) and the Transcripted and TaqMan mRNA assay primers for miR-146b and miR-155 (Tiangen, China) were used for quantitative real-time RT-PCR analysis. Reactions were carried out using the Applied Biosystems 7500 Fast Real-Time PCR System (Life Technologies, USA), and displayed threshold cycles (Ct) 35 were excluded from the analysis. The expressions of miRNA values were calculated using snoRNA234 as an endogenous control by the $2^{-\Delta\Delta CT}$ relative quantification method [22]. miRNA expression was analyzed as fold changes.

Statistical Analysis

All results are expressed as the mean ± standard deviation (SD). Data were analyzed using the Mann-Whitney *U* test or one-way ANOVA followed by Tukey-Kramer multiple tests. SPSS 16.0 (IBM, USA) was used for

Table 2. Primer Sequences Used for Quantitative Real-Time PCR

Primer	Forward	Reverse
LOX-1	TGAAGCCTGCGAATGACGAG	GTCACTGACAACACCCAGGCAGAG
COX-2	TGCCAGGCTGAACTTCGAAAC	GCTCACGAGGCCACTGATACCTA
FASN	AGCACTGCCTTCGGTTCAGTC	AAGAGCTGTGGAGGCCACTTG
HMG-COA	TGTCCTTGATGGCAGCCTTG	CGCGCTTCAGTTCAGTGTCAG
CRP	GAACTGGCGGGCACTGAACTA	GGAGGTGCTTCAGGGTTCACA
CCL-2	GCATCCACGTGTTGGCTCA	CTCCAGCCTACTCATTGGGATCA
CD40	GTAAGCGAAGCCAACAGTAATGC	CCGATTAGAGCAGAAGGTGACTTG
IL-1β	CTATACCTGTCCTGTGTAATGAAAGA	TCTGCTTGTGAGGTGCTGATGTA
IL-6	TAGCTACCTGGAGTACATGAAGAACA	TGGTCCTTAGCCACTCCTTCTG
TNF-α	AGGCGGTGCCTATGTCTCAG	GCCATTTGGGAACTTCTCATC
MMP-2	GATAACCTGGATGCCGTCGTG	CTTCACGCTCTTGAGACTTTGGTTC
MMP-9	GCCCTGGAACTCACACGACA	TTGGAAACTCACACGCCAGAAG
GAPDH	TGTGTCCGTCGTGGATCTGA	TTGCTGTTGAAGTCGCAGGAG

analysis. $P < 0.05$ was considered to indicate statistical significance.

RESULTS

Atherosclerotic Plaques in Aortic Sinus

The atherosclerotic plaque in the cryosections of the aortic sinus was examined by Oil Red O staining. The percentage of the lumen of the proximal aorta occupied by atherosclerotic plaque was higher in the *P. gingivalis*-challenged mice compared with the PBS-inoculated mice (Fig. 2a, b, PBS: $5.99 \pm 2.02\%$ *vs.* *P. gingivalis*: $10.54 \pm 1.78\%$; $P < 0.01$). In contrast, the TSA-treated group presented smaller atherosclerotic plaque lesions caused by *P. gingivalis* infection (Fig. 2a, b, *P. gingivalis*: $10.54 \pm 1.78\%$ *vs.* *P. gingivalis* + TSA: $8.71 \pm 1.66\%$, $P < 0.05$).

Atherosclerosis-Associated Factors in the Serum

To evaluate whether TSA inhibits the progression of atherosclerosis, atherosclerosis-associated factors were measured in the serum using the Mouse Atherosclerosis Antibody Array C1. *P. gingivalis* challenge increased the serum levels of basic fibroblast growth factor (bFGF) ($P < 0.05$), CD40 ($P < 0.01$), eotaxin-1 ($P < 0.01$), interferon-γ (IFN-γ) ($P < 0.05$), IL-1β ($P < 0.05$), IL-6 ($P < 0.05$), regulated on activation, normal T Cell expressed and secreted (RANTES) ($P < 0.01$), TNF-α ($P < 0.01$), and vascular endothelial growth factor (VEGF) ($P < 0.01$) compared with the PBS-inoculated mice. The expression of bFGF ($P < 0.05$), CD40 ($P < 0.01$), eotaxin-1 ($P < 0.01$), granulocyte-colony stimulating factor (G-CSF) ($P < 0.05$), IFN-γ ($P < 0.01$), IL-1β ($P < 0.01$), IL-6 ($P < 0.01$), monocyte chemoattractant protein-1 (MCP-1) ($P < 0.01$), macrophage inflammatory protein-3α (MIP-3α) ($P < 0.01$), RANTES ($P < 0.05$), TNF-α ($P < 0.05$), and VEGF ($P < 0.01$) was decreased in TSA-treated mice compared with the *P. gingivalis*-challenged mice (Fig. 3).

Inflammatory Cytokines and Oxidative Stress Markers in the Serum

Cytokine ELISA was performed on serum samples to characterize the magnitude of the atherosclerotic risk factors in different groups. Compared to the PBS-inoculated mice, the *P. gingivalis*-challenged mice showed high levels of IL-1β (Fig. 4a, 240.6 ± 35 *vs.* 124.7 ± 50.4 pg mL^{-1}, $P < 0.01$), IL-6 (Fig. 4b, 287.9 ± 85.5 *vs.* 146.4 ± 41.2 pg mL^{-1}, $P < 0.01$), TNF-α (Fig. 4c, 767.8 ± 101.2 *vs.* 600.3 ± 39.1 pg mL^{-1}, $P < 0.01$), CRP (Fig. 4e, 615.6 ± 57.7 *vs.* 451.2 ± 22 μg L^{-1}, $P < 0.01$), ox-LDL (Fig. 4f, 7.6 ± 1.0 *vs.* 5.3 ± 0.4 μmol mL^{-1}, $P < 0.01$), HDL (Fig. 4g, 57.4 ± 3.9 *vs.* 71.9 ± 14.8 μmol mL^{-1},
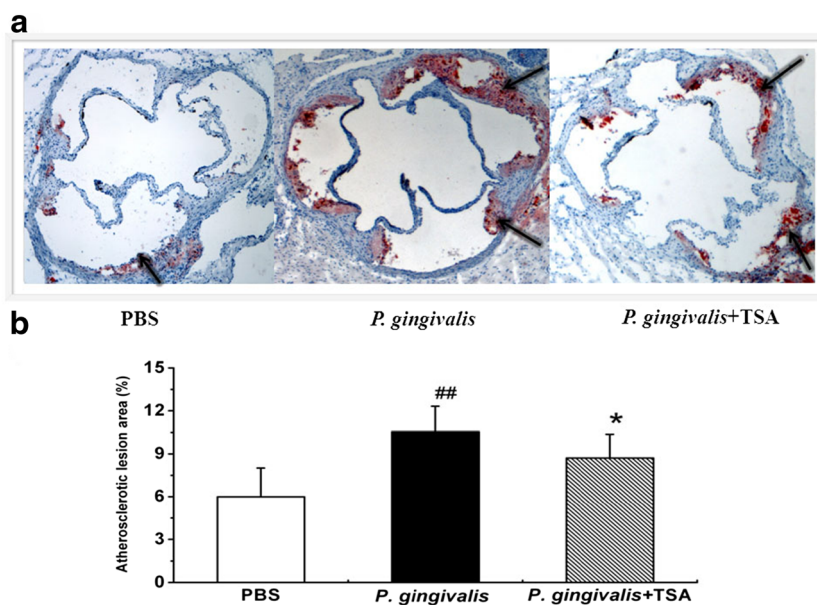

Fig. 2. Lipid deposition stained with Oil Red O. *Arrows* indicate typical lipid deposition of atherosclerosis area in the aortic sinus of ApoE$^{-/-}$ mice from different groups (original magnification ×100) (**a**). The percentage of the aortic sinus occupied by lesions is shown at 16 weeks (**b**). The data represent the mean ± SD ($n = 8$). $^{\#\#}P < 0.01$ compared with the PBS-inoculated group; $^{*}P < 0.05$ compared with the *Porphyromonas gingivalis*-challenged group.
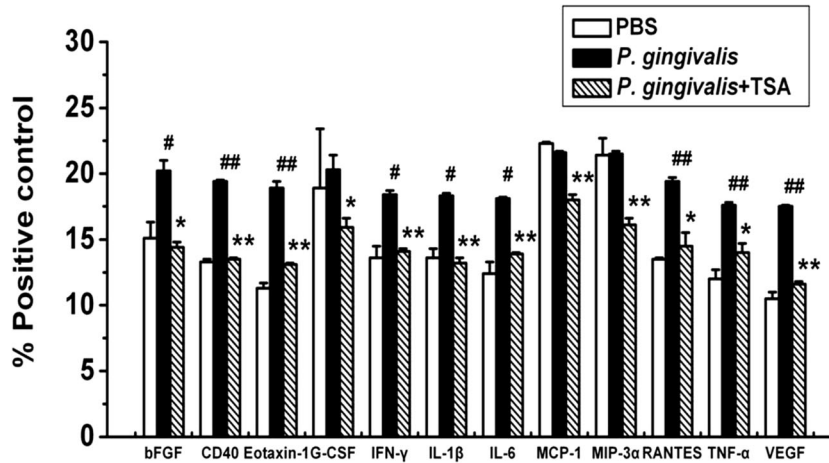
Fig. 3. Cytokine expression tested by the Mouse Atherosclerosis Antibody Array. Configuration of atherosclerosis risk factors from *Porphyromonas gingivalis*-challenged and TSA-treated serum samples collected at 16 weeks. The expression of each cytokine is presented as the percentage of the positive control. The data present the mean ± SD of three independent experiments on each sample. [#]$P < 0.05$, [##]$P < 0.01$ compared with the PBS-inoculated group. *$P < 0.05$, **$P < 0.01$ compared with the *P. gingivalis*-challenged group.

$P < 0.05$), and LDL/VLDL (Fig. 4h, 32.4 ± 5.2 *vs.* $25.4 \pm 7.6\ \mu\text{mol mL}^{-1}$, $P < 0.05$); the exception was IL-12

(Fig. 4d, PBS: $119.2 \pm 14.8\ \text{pg mL}^{-1}$ *vs. P. gingivalis*: $128.1 \pm 17.0\ \text{pg mL}^{-1}$, $P > 0.05$).
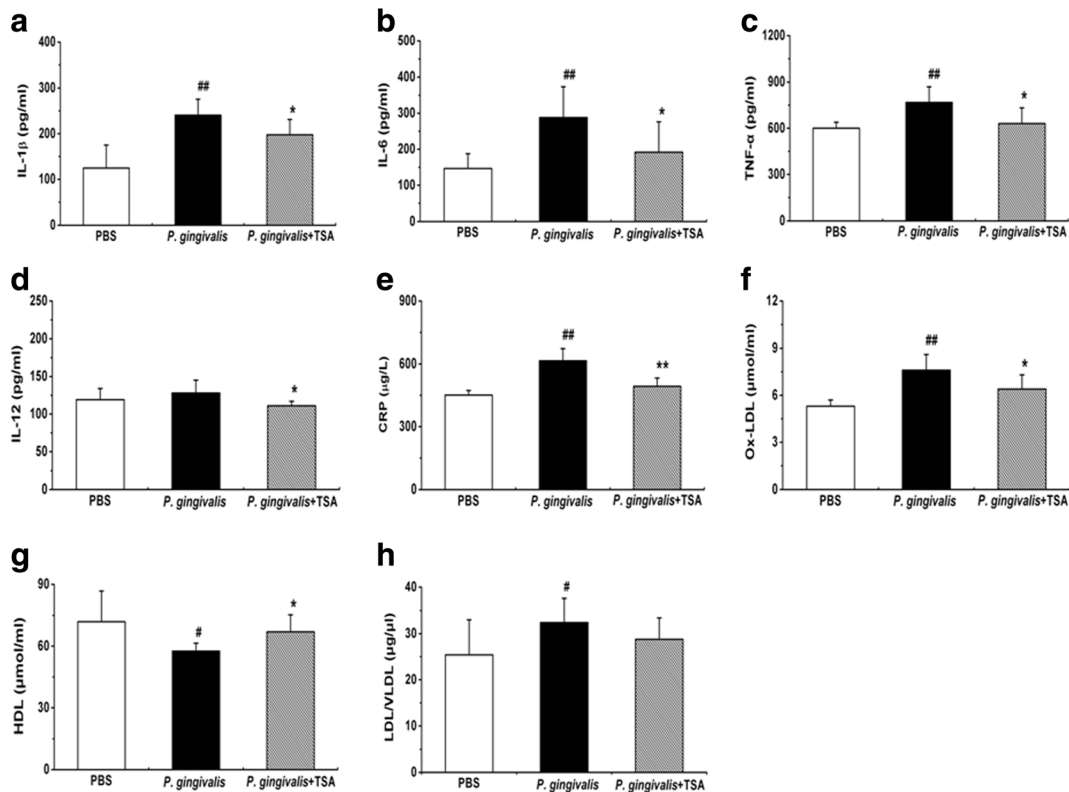

Fig. 4. Serum cytokines detected by ELISA assay. Serum levels of inflammatory cytokines IL-1β, IL-6, TNF-α, and IL-12 (**a**–**d**), and inflammatory marker CRP combined with oxidative mediators ox-LDL, HDL, and LDL/VLDL (**e**–**h**) in samples gathered at 16 weeks, were detected by ELISA assay. The data represent the mean ± SD ($n = 8$). [#]$P < 0.05$, [##]$P < 0.01$ compared with the PBS-inoculated group. *$P < 0.05$, **$P < 0.01$ compared with the *Porphyromonas gingivalis*-challenged group.

In contrast, TSA treatment decreased IL-1β (Fig. 4a, 197.6 ± 33.6 *vs.* 240.6 ± 35 pg mL^{-1}, $P < 0.05$), IL-6 (Fig. 4b, 191.9 ± 84.3 *vs.* 287.9 ± 85.5 pg mL^{-1}, $P < 0.05$), TNF-α (Fig. 4c, 630.9 ± 101.7 *vs.* 767.8 ± 101.2 pg mL^{-1}, $P < 0.05$), IL-12 (Fig. 4d, 111 ± 6.0 *vs.* 128.1 ± 17 pg mL^{-1}, $P < 0.05$), CRP (Fig. 4e, 493.1 ± 39.5 *vs.* 615.6 ± 57.7 µg L^{-1}, $P < 0.01$), ox-LDL (Fig. 4f, 6.4 ± 0.9 *vs.* 7.6 ± 1.0 µmol mL^{-1}, $P < 0.05$), and HDL (Fig. 4g, 67.0 ± 8.3 *vs.* 57.4 ± 3.9 µmol mL^{-1}, $P < 0.05$). However, LDL/VLDL was not statistically significant (Fig. 4h, *P. gingivalis*: 32.4 ± 5.2 µmol mL^{-1} *vs.* *P. gingivalis* + TSA: 28.8 ± 4.6 µmol mL^{-1}, $P > 0.05$).

Inflammatory Cytokines and Oxidative Mediators in Heart, Aorta, and Liver Tissues

To examine the involvement of various inflammatory and oxidative mediators in atherosclerosis activated by *P. gingivalis* infection, the gene expression of inflammatory cytokines and oxidative markers was detected by real-time PCR in the heart, aorta, and liver tissues. In the heart tissue, *P. gingivalis* infection elevated the expression of CCL-2 ($P < 0.01$), CD40 ($P < 0.01$), IL-1β ($P < 0.01$), IL-6 ($P < 0.01$), TNF-α ($P < 0.01$), matrix metalloproteinase (MMP)-2 $P < 0.01$), and MMP-9 ($P < 0.05$), as well as the oxidative mediators lectin-like ox-LDL receptor-1 (LOX-1) ($P < 0.05$) and cyclooxygenase-2 (COX-2) ($P < 0.05$), compared to the PBS-inoculated mice. In contrast, the TSA-treated group showed significantly decreased expression of CCL-2 ($P < 0.05$), CD40 ($P < 0.05$), IL-1β ($P < 0.05$), IL-6 ($P < 0.05$), TNF-α ($P < 0.05$), and MMP-2 ($P < 0.01$) (Fig. 5a).

In the aorta (Fig. 5b), *P. gingivalis* induced an increase in the expression of CCL-2 ($P < 0.01$), CD40 ($P < 0.01$), IL-1β ($P < 0.01$), IL-6 ($P < 0.01$), TNF-α ($P < 0.01$), MMP-2 ($P < 0.05$), MMP-9 ($P < 0.05$), and LOX-1 ($P < 0.01$), but not COX-2. Compared to the *P. gingivalis*-challenged group, TSA treatment reduced the expression of CCL-2 ($P < 0.05$), CD40 ($P < 0.05$), IL-1β ($P < 0.05$), IL-6 ($P < 0.05$), TNF-α ($P < 0.05$), and MMP-2 ($P < 0.05$).

In addition, although TSA treatment significantly decreased the expression of CRP ($P < 0.05$) activated by *P. gingivalis* infection, no significant differences were observed between the *P. gingivalis*-challenged and TSA-treated groups for fatty acid synthase (FASN) and 3-hydroxy-3-methylglutaryl coenzyme A (HMG-COA) from liver samples (Fig. 5c).

MicroRNA Expression in the Heart Tissue

The relative expression of miR-146b was elevated by *P. gingivalis* infection in ApoE$^{-/-}$ mice ($P < 0.01$), and downregulated by TSA treatment in the heart tissue ($P < 0.01$). Similarly, miR-155 relative expression showed a marked increase in *P. gingivalis*-challenged mice ($P < 0.01$), and then was significantly decreased by TSA ($P < 0.05$) (Fig. 6).

DISCUSSION

P. gingivalis is a major pathogen involved in the inflammatory responses of periodontal disease. Inflammatory responses caused by *P. gingivalis* infection also promote the development of atherosclerosis by injuring the vascular endothelium [23]. Many studies have shown that *P. gingivalis* infection accelerated the progression of atherosclerosis in humans [24] and animal models [9, 19]. Furthermore, studies have revealed that *P. gingivalis* not only invades vascular endothelial cells [7] but also activates immune cells such as dendritic cells, T cells, and monocytes to induce inflammatory responses in the cardiovascular system [25].

Therefore, the present study showed that *P. gingivalis* infection accelerated atherosclerotic plaque development in ApoE$^{-/-}$ mice, and that this was associated with increased serum of the atherosclerotic factors bFGF, eotaxin-1, G-CSF, MCP-1, MIP-3α, IFN-γ, IL-1β, IL-6, TNF-α, CD40, VEGF, and RANTES compared with PBS-inoculated mice. Furthermore, the serum levels of the inflammatory cytokines IL-1β, IL-6, IL-12, and TNF-α, and of the inflammatory marker CRP, and the mRNA expressions of IL-1β, IL-6, TNF-α, CRP, MMP-2, MMP-9, CCL-2, and CD40 in the heart and aorta tissues were increased in *P. gingivalis*-challenged mice. On the other hand, the oxidative mediators ox-LDL, LDL/VLDL, LOX-1, COX-2, FASN, and HMG-COA were only marginally upregulated by *P. gingivalis* infection. In addition, the relative expression of miR-146b and miR-155 showed a marked increase in *P. gingivalis*-challenged mice. Many studies have reported that *P. gingivalis* can increase the inflammatory mediators IL-1β, IL-6, IL-12, TNF-α, and MCP-1 and accelerate the development of atherosclerosis [26, 27]. *P. gingivalis* invasion also
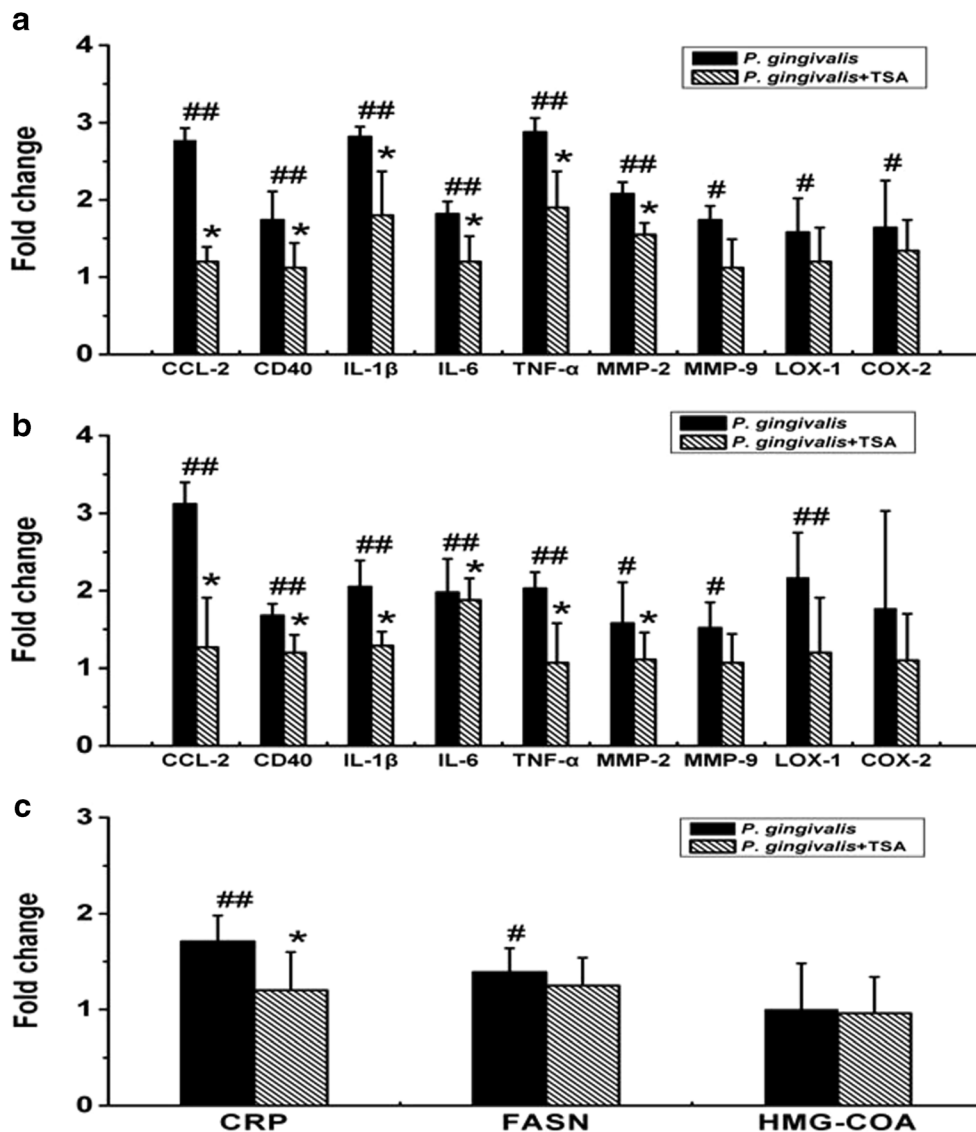
Fig. 5. mRNA expressions of inflammatory and oxidative mediators obtained by quantitative real-time PCR. The relative mRNA expressions of inflammatory and oxidative mediators were obtained after normalization to GAPDH by real-time PCR in heart (**a**), aorta (**b**), and liver (**c**) tissues. Data are expressed as the fold increases in the mRNA level compared with the PBS-inoculated group or *Porphyromonas gingivalis*-challenged group. Values represent the mean ± SD ($n = 8$). #$P < 0.05$, ##$P < 0.01$ compared with the PBS-inoculated group. *$P < 0.05$, **$P < 0.01$ compared with the *P. gingivalis*-challenged group.

upregulate M-CSF, G-CSF, IFN-γ, IL-1β, IL-13, CD40, RANTES, CRP, MMP-2, and MMP-9, inducing the host immune response to accelerate atherosclerotic lesion formation [8, 10, 28]. Recently, *P. gingivalis* has been shown to activate the expression of TLR-2, TLR-4, TNF-α, CRP, IL-6, MMP-9, and MCP-1 through the nuclear factor kappa-B (NF-κB), p65, p38-MAPK, and JNK signaling pathways in a rabbit model [9]. On the other hand, several reports have indicated that *P. gingivalis* exacerbates ox-LDL- and TNF-α-induced endothelial injury and

positively correlates with LDL-C levels [29]. One of our previous studies also demonstrated that *P. gingivalis* infection with high-fat diet induced atherosclerotic lesions and elevated the expression of inflammatory cytokines and oxidative mediators in ApoE$^{-/-}$ mice [6]. In an animal study of GroEL from *P. gingivalis*, GroEL elevated ICAM-1, VCAM-1, LOX-1, and TLR4 expression in the aortas of high-cholesterol diet-fed wild-type C57BL/6 mice [30]. Moreover, *P. gingivalis* lipopolysaccharide (LPS) increased the expression of COX-2 mRNA in
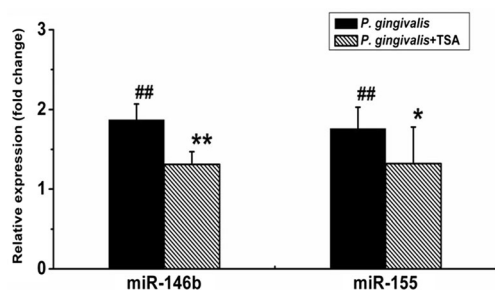
Fig. 6. miR-146b and miR-155 analyzed by real-time PCR. The relative expression of miR-146b and miR-155 was analyzed by real-time PCR in PBS-inoculated, *Porphyromonas gingivalis*-challenged, and TSA-treated mice at 16 weeks. Data are expressed as the fold change increases in the *P. gingivalis*-challenged group compared with the PBS-inoculated group, and decreases in the TSA-treated group after normalization to snoRNA234. Values represent the mean ± SD ($n = 8$). $^{##}P < 0.01$ compared with the PBS-inoculated group. $^{*}P < 0.05$, $^{**}P < 0.01$ compared with the *P. gingivalis*-challenged group.

the aortic root of ApoE$^{-/-}$ mice [31]. In brief, *P. gingivalis* and its virulence factors play important roles in inflammation and oxidative stress, and thus accelerate the development of atherosclerosis.

Danshen is widely used in traditional Chinese medicine for the treatment of cardiovascular diseases such as myocardial infarction (MI), atherosclerosis, and thromboangiitis obliterans [32]. TSA, a major component of Danshen, has anti-inflammatory, anti-oxidative, and cardioprotective effects [15, 16, 33]. The drug named Fufang Danshen is listed in the Chinese Pharmacopoeia and has completed phase III clinical trials for evaluating its efficacy and safety in patients with chronic stable angina pectoris in the USA (no. NCT01659580) [34]. Most studies revealed the anti-oxidative effect of TSA for preventing cardiovascular disease, but studies about the anti-inflammatory effects of TSA in atherosclerosis are limited. With this goal in mind, the present study showed that *P. gingivalis* accelerated the progression of atherosclerosis, and that this could be prevented by TSA treatment.

In this study, TSA attenuated the development of atherosclerotic lesions in ApoE$^{-/-}$ mice associated with reducing the inflammatory biomarkers CRP, IL-1β, IL-6, IL-12, MMP-2, MMP-9, CCL-2, CD40, and TNF-α, and with slightly decreasing the oxidative mediators ox-LDL, COX-2, and LOX-1 compared with the *P. gingivalis*-challenged mice. A previous study revealed that TSA decreased the serum ox-LDL levels in ApoE$^{-/-}$ mice and reduced ox-LDL production by downregulation of scavenger receptors,

namely scavenger receptor-A (SR-A) and CD36 [20]. Other studies also demonstrated that TSA stabilized the plaque by weakening the impact of ox-LDL-induced ICAM-1 and MMP-9 expression in endothelial cells, both *in vivo* and *in vitro* [15, 35]. TSA could downregulate ox-LDL through the inhibition of LOX-1 expression, and this might in turn contribute to the amelioration of atherosclerosis [36], supporting the present study. TSA did not affect the serum lipid levels but reduced the levels of HDL middle subfractions and increased the levels of HDL large subfractions [37]. On the other hand, TSA had no effect on the lipid synthesis-related factors HMG-COA and FASN. There are many enzymes involved in the regulation of lipid metabolism [38], but only two of them has been examined in this present study. Future work should examine the effects of TSA on a comprehensive panel of enzymes involved in the synthesis of lipids.

TSA has been suggested to regulate a variety of inflammatory mediators. The interplay of serum CRP with LOX-1 and ox-LDL is involved in the endothelial dysfunction that leads to atherosclerosis [39]. Pro-inflammatory factors, such as TNF-α, CRP, and IL-1, could increase LOX-1 expression [40], which is also elevated by *P. gingivalis* infection and downregulated by TSA in the present study. Another study suggested that TSA could weaken the impact of ox-LDL-induced stimulation of ICAM-1 and MMP-9 expression in endothelial cells [35]. Consistent with our data, TSA regulated the expression of IL-1β, IL-6, TNF-α, CD40, ICAM-1, and VCAM-1, all of which were regulated by NF-κB and related to endothelial dysfunction induced by monocytes/macrophages [41–43]. Moreover, Xu *et al.* also revealed that TSA obviously inhibited the expression of NF-κB, as well as decreased inflammatory cytokine levels of MCP-1, IL-6, and TNF-α in ApoE$^{-/-}$ mice [44]. CD40, the key regulator of the inflammation process and involved in all stages of atherosclerosis, could be decreased by TSA in a human umbilical vein endothelial cell (HUVEC) line damaged by H$_2$O$_2$ [45]. The expression of IL-12 and IFN-γ was strongly inhibited by TSA in LPS-stimulated macrophages [46], as was also demonstrated by our study in ApoE$^{-/-}$ mice with *P. gingivalis* infection.

MMPs promote inflammation in the injured vascular wall and the formation of plaque by infiltration of T cells, macrophages, and SMCs [47]. In

particular, MMP-2 and MMP-9 have been identified as major proteinases degrading collagens during atherosclerotic plaque formation and instability [48]. TSA inhibited MMP-2 and MMP-9 expression/activity in atherosclerotic plaques from rabbits given a high-fat diet [49]. In the present study, we demonstrated that the levels of MMP-2 were reduced by TSA without affecting MMP-9 expression in heart and aorta tissues. Fang *et al*. revealed that TSA at a high dose (70 mg kg^{-1} day^{-1}) exerted suppressive effects on the gene expression of MMP-9 in rats with renovascular hypertension [50]. We speculated that TSA at 60 mg kg^{-1} day^{-1} could attenuate the development of atherosclerosis through an anti-inflammatory effect. Clinical studies have reported that the miRNA levels from blood were significantly altered in patients with cardiovascular diseases. The expression of miR-146a/b in monocytes is strongly affected by pro-inflammatory stimuli such as LPS through NF-κB-dependent mechanisms [51].

Studies have shown that miR-146b was expressed by endothelial cells upon exposure to pro-inflammatory cytokines, and miR-155 was expressed by ox-LDL to regulate foam cell formation; both played crucial roles in the development of atherosclerosis [52, 53]. miR-155 expressed in monocytes shows the most pronounced changes after LPS, IFN-γ, or TNF-α stimulation in an NF-κB-dependent manner and has opposing effects on TNF-α production [54]. On the other hand, miR-155 could enhance the translation of TNF-α by affecting the stability of transcription of IKKε, FADD, and Ripk1. Both miR-146b and miR-155 have been reported to correlate with cardiovascular diseases [55]. Therefore, TSA may exert an atherogenic effect associated with inhibiting the levels of miR-146b and miR-155, as observed in the present study.

CONCLUSIONS

In conclusion, *P. gingivalis* infection induced inflammatory responses and played a critical role in the development of atherosclerosis in ApoE$^{-/-}$ mice. This could be prevented by TSA treatment. TSA decreased the expression of inflammatory mediators associated with the progression of atherosclerosis. TSA could be useful for the prevention of pathogen-accelerated atherosclerosis through anti-inflammatory and anti-oxidative effects.

REFERENCES

1. Libby, P., P.M. Ridker, and G.K. Hansson. 2011. Progress and challenges in translating the biology of atherosclerosis. *Nature* 473 (7347): 317–325. doi:10.1038/nature10146.
2. Beck, J., R. Garcia, G. Heiss, P.S. Vokonas, and S. Offenbacher. 1996. Periodontal disease and cardiovascular disease. *Journal of Periodontology* 67 (10 Suppl): 1123–1137. doi:10.1902/jop.1996.67.10s.1123.
3. Grossi, S.G., and R.J. Genco. 1998. Periodontal disease and diabetes mellitus: A two-way relationship. *Annals of Periodontology* 3 (1): 51–61. doi:10.1902/annals.1998.3.1.51.
4. Straka, M., M. Straka-Trapezanlidis, J. Deglovic, and I. Varga. 2015. Periodontitis and osteoporosis. *Neuro Endocrinology Letters* 36 (5): 401–406.
5. Bahekar, A.A., S. Singh, S. Saha, J. Molnar, and R. Arora. 2007. The prevalence and incidence of coronary heart disease is significantly increased in periodontitis: A meta-analysis. *American Heart Journal* 154 (5): 830–837. doi:10.1016/j.ahj.2007.06.037.

6. Cai, Y., T. Kurita-Ochiai, T. Hashizume, and M. Yamamoto. 2013. Green tea epigallocatechin-3-gallate attenuates Porphyromonas gingivalis-induced atherosclerosis. *Pathogens and disease* 67 (1): 76–83. doi:10.1111/2049-632X.12001.

7. Champaiboon, C., M. Poolgesorn, W. Wisitrasameewong, N. Sa-Ard-Iam, P. Rerkyen, and R. Mahanonda. 2014. Differential inflammasome activation by Porphyromonas gingivalis and cholesterol crystals in human macrophages and coronary artery endothelial cells. *Atherosclerosis* 235 (1): 38–44. doi:10.1016/j.atherosclerosis.2014.04.007.

8. Chukkapalli, S.S., I.M. Velsko, M.F. Rivera-Kweh, D. Zheng, A.R. Lucas, and L. Kesavalu. 2015. Polymicrobial oral infection with four periodontal bacteria orchestrates a distinct inflammatory response and atherosclerosis in ApoE null mice. *PloS One* 10 (11): e0143291. doi:10.1371/journal.pone.0143291.

9. Lin, G., S. Chen, L. Lei, X. You, M. Huang, L. Luo, Y. Li, X. Zhao, and F. Yan. 2015. Effects of intravenous injection of Porphyromonas gingivalis on rabbit inflammatory immune response and atherosclerosis. *Mediators of Inflammation* 2015: 364391. doi:10.1155/2015/364391.

10. Pan, S., L. Lei, S. Chen, H. Li, and F. Yan. 2014. Rosiglitazone impedes Porphyromonas gingivalis-accelerated atherosclerosis by downregulating the TLR/NF-kappaB signaling pathway in atherosclerotic mice. *International Immunopharmacology* 23 (2): 701–708. doi:10.1016/j.intimp.2014.10.026.

11. Deshpande, R.G., M.B. Khan, and C.A. Genco. 1998. Invasion of aortic and heart endothelial cells by Porphyromonas gingivalis. *Infection and Immunity* 66 (11): 5337–5343.

12. Roth, G.A., K. Aumayr, M.B. Giacona, P.N. Papapanou, A.M. Schmidt, and E. Lalla. 2009. Porphyromonas gingivalis infection and prothrombotic effects in human aortic smooth muscle cells. *Thrombosis Research* 123 (5): 780–784. doi:10.1016/j.thromres.2008.07.008.

13. Libby, P., P.M. Ridker, and A. Maseri. 2002. Inflammation and atherosclerosis. *Circulation* 105 (9): 1135–1143.

14. Cheng, T.O. 2006. Danshen: A popular Chinese cardiac herbal drug. *Journal of the American College of Cardiology* 47 (7): 1498; author reply 1499–1500. doi:10.1016/j.jacc.2006.01.001.

15. Tang, F., X. Wu, T. Wang, P. Wang, R. Li, H. Zhang, J. Gao, S. Chen, L. Bao, H. Huang, and P. Liu. 2007. Tanshinone II A attenuates atherosclerotic calcification in rat model by inhibition of oxidative stress. *Vascular Pharmacology* 46 (6): 427–438. doi:10.1016/j.vph.2007.01.001.

16. Chen, Z., and H. Xu. 2014. Anti-inflammatory and immunomodulatory mechanism of Tanshinone IIA for atherosclerosis. *Evidence-based complementary and alternative medicine : eCAM* 2014: 267976. doi:10.1155/2014/267976.

17. Gong, Z., C. Huang, X. Sheng, Y. Zhang, Q. Li, M.W. Wang, L. Peng, and Y.Q. Zang. 2009. The role of Tanshinone IIA in the treatment of obesity through peroxisome proliferator-activated receptor gamma antagonism. *Endocrinology* 150 (1): 104–113. doi:10.1210/en.2008-0322.

18. Gao, S., Z. Liu, H. Li, P.J. Little, P. Liu, and S. Xu. 2012. Cardiovascular actions and therapeutic potential of tanshinone IIA. *Atherosclerosis* 220 (1): 3–10. doi:10.1016/j.atherosclerosis.2011.06.041.

19. Hayashi, C., J. Viereck, N. Hua, A. Phinikaridou, A.G. Madrigal, F.C. Gibson 3rd, J.A. Hamilton, and C.A. Genco. 2011. Porphyromonas gingivalis accelerates inflammatory atherosclerosis in the innominate artery of ApoE deficient mice. *Atherosclerosis* 215 (1): 52–59. doi:10.1016/j.atherosclerosis.2010.12.009.

20. Tang, F.T., Y. Cao, T.Q. Wang, L.J. Wang, J. Guo, X.S. Zhou, S.W. Xu, W.H. Liu, P.Q. Liu, and H.Q. Huang. 2011. Tanshinone IIA attenuates atherosclerosis in ApoE($^{-/-}$) mice through down-

regulation of scavenger receptor expression. *European Journal of Pharmacology* 650 (1): 275–284. doi:10.1016/j.ejphar.2010.07.038.

21. Paigen, B., A. Morrow, P.A. Holmes, D. Mitchell, and R.A. Williams. 1987. Quantitative assessment of atherosclerotic lesions in mice. *Atherosclerosis* 68 (3): 231–240.

22. Livak, K.J., and T.D. Schmittgen. 2001. Analysis of relative gene expression data using real-time quantitative PCR and the 2(−Delta Delta C(T)) method. *Methods* 25 (4): 402–408. doi:10.1006/meth.2001.1262.

23. Cutler, C.W., J.R. Kalmar, and C.A. Genco. 1995. Pathogenic strategies of the oral anaerobe, Porphyromonas gingivalis. *Trends in Microbiology* 3 (2): 45–51.

24. Mahendra, J., L. Mahendra, V.M. Kurian, K. Jaishankar, and R. Mythilli. 2010. 16S rRNA-based detection of oral pathogens in coronary atherosclerotic plaque. *Indian journal of dental research : official publication of Indian Society for Dental Research* 21 (2): 248–252. doi:10.4103/0970-9290.66649.

25. Wang, Q., X. Zhou, and D. Huang. 2009. Role for Porphyromonas gingivalis in the progression of atherosclerosis. *Medical Hypotheses* 72 (1): 71–73. doi:10.1016/j.mehy.2008.04.030.

26. Shaddox, L.M., P.F. Goncalves, A. Vovk, N. Allin, H. Huang, W. Hou, I. Aukhil, and S.M. Wallet. 2013. LPS-induced inflammatory response after therapy of aggressive periodontitis. *Journal of Dental Research* 92 (8): 702–708. doi:10.1177/0022034513495242.

27. Gibson, F.C. 3rd, T. Ukai, and C.A. Genco. 2008. Engagement of specific innate immune signaling pathways during Porphyromonas gingivalis induced chronic inflammation and atherosclerosis. *Frontiers in bioscience : a journal and virtual library* 13: 2041–2059.

28. Hajishengallis, G., H. Sojar, R.J. Genco, and E. DeNardin. 2004. Intracellular signaling and cytokine induction upon interactions of Porphyromonas gingivalis fimbriae with pattern-recognition receptors. *Immunological Investigations* 33 (2): 157–172.

29. Bugueno, I.M., Y. Khelif, N. Seelam, D.N. Morand, H. Tenenbaum, J.L. Davideau, and O. Huck. 2016. Porphyromonas gingivalis differentially modulates cell death profile in ox-LDL and TNF-alpha pre-treated endothelial cells. *PloS One* 11 (4): e0154590. doi:10.1371/journal.pone.0154590.

30. Huang, C.Y., C.M. Shih, N.W. Tsao, Y.W. Lin, C.C. Shih, K.H. Chiang, S.K. Shyue, Y.J. Chang, C.K. Hsieh, and F.Y. Lin. 2016. The GroEL protein of Porphyromonas gingivalis regulates atherogenic phenomena in endothelial cells mediated by upregulating toll-like receptor 4 expression. *American Journal of Translational Research* 8 (2): 384–404.

31. Gitlin, J.M., and C.D. Loftin. 2009. Cyclooxygenase-2 inhibition increases lipopolysaccharide-induced atherosclerosis in mice. *Cardiovascular Research* 81 (2): 400–407. doi:10.1093/cvr/cvn286.

32. Zhou, L., Z. Zuo, and M.S. Chow. 2005. Danshen: An overview of its chemistry, pharmacology, pharmacokinetics, and clinical use. *Journal of Clinical Pharmacology* 45 (12): 1345–1359. doi:10.1177/0091270005282630.

33. Zhou, G.Y., B.L. Zhao, J.W. Hou, G.E. Ma, and W.J. Xin. 1999. Protective effects of sodium tanshinone IIA sulphonate against adriamycin-induced lipid peroxidation in mice hearts in vivo and in vitro. *Pharmacological Research* 40 (6): 487–491. doi:10.1006/phrs.1999.0545.

34. Tasly Pharmaceuticals, Inc. 2012. Phase III Trial of Dantonic® (T89) Capsule to Prevent and Treat Stable Angina (CAESA). http://clinicaltrials.gov/ct2/show/NCT01659580?term=Tasly&rank=3. Accessed 7 March 2017.

35. Ju, H., W.L. Cheng, and X. Dong. 2005. Effect of salvia miltiorrhiza on the expression of matrix metalloproteinase 9 and intercellular adhesive moleculer-1 induced by oxidized low-density lipoprotein in human umbilical vein endothelial cells. *Journal of China-Japan Friendship Hospital* 19 (4): 230–232.

36. Chen, W., F. Tang, B. Xie, S. Chen, H. Huang, and P. Liu. 2012. Amelioration of atherosclerosis by tanshinone IIA in hyperlipidemic rabbits through attenuation of oxidative stress. *European Journal of Pharmacology* 674 (2–3): 359–364. doi:10.1016/j.ejphar.2011.10.040.

37. Jia, L.Q., N. Zhang, Y. Xu, W.N. Chen, M.L. Zhu, N. Song, L. Ren, H.M. Cao, J.Y. Wang, and G.L. Yang. 2016. Tanshinone IIA affects the HDL subfractions distribution not serum lipid levels: Involving in intake and efflux of cholesterol. *Archives of Biochemistry and Biophysics* 592: 50–59. doi:10.1016/j.abb.2016.01.001.

38. Ye, J., and R.A. DeBose-Boyd. 2011. Regulation of cholesterol and fatty acid synthesis. *Cold Spring Harbor Perspectives in Biology* 3 (7). doi:10.1101/cshperspect.a004754.

39. Li, L., N. Roumeliotis, T. Sawamura, and G. Renier. 2004. C-reactive protein enhances LOX-1 expression in human aortic endothelial cells: Relevance of LOX-1 to C-reactive protein-induced endothelial dysfunction. *Circulation Research* 95 (9): 877–883. doi:10.1161/01.RES.0000147309.54227.42.

40. Xu, S., S. Ogura, J. Chen, P.J. Little, J. Moss, and P. Liu. 2013. LOX-1 in atherosclerosis: Biological functions and pharmacological modifiers. *Cellular and molecular life sciences : CMLS* 70 (16): 2859–2872. doi:10.1007/s00018-012-1194-z.

41. Jang, S.I., S.I. Jeong, K.J. Kim, H.J. Kim, H.H. Yu, R. Park, H.M. Kim, and Y.O. You. 2003. Tanshinone IIA from Salvia miltiorrhiza inhibits inducible nitric oxide synthase expression and production of TNF-alpha, IL-1beta and IL-6 in activated RAW 264.7 cells. *Planta Medica* 69 (11): 1057–1059. doi:10.1055/s-2003-45157.

42. Jang, S.I., H.J. Kim, Y.J. Kim, S.I. Jeong, and Y.O. You. 2006. Tanshinone IIA inhibits LPS-induced NF-kappaB activation in RAW 264.7 cells: Possible involvement of the NIK-IKK, ERK1/2, p38 and JNK pathways. *European Journal of Pharmacology* 542 (1–3): 1–7. doi:10.1016/j.ejphar.2006.04.044.

43. Ling, S., A. Dai, Z. Guo, and P.A. Komesaroff. 2008. A preparation of herbal medicine Salvia miltiorrhiza reduces expression of intercellular adhesion molecule-1 and development of atherosclerosis in apolipoprotein E-deficient mice. *Journal of Cardiovascular Pharmacology* 51 (1): 38–44. doi:10.1097/FJC.0b013e31815a9575.

44. Xu, S., P.J. Little, T. Lan, Y. Huang, K. Le, X. Wu, X. Shen, H. Huang, Y. Cai, F. Tang, H. Wang, and P. Liu. 2011. Tanshinone II-A attenuates and stabilizes atherosclerotic plaques in apolipoprotein-E knockout mice fed a high cholesterol diet. *Archives of Biochemistry and Biophysics* 515 (1–2): 72–79. doi:10.1016/j.abb.2011.08.006.

45. Lin, R., W.R. Wang, J.T. Liu, G.D. Yang, and C.J. Han. 2006. Protective effect of tanshinone IIA on human umbilical vein endothelial cell injured by hydrogen peroxide and its mechanism. *Journal of Ethnopharmacology* 108 (2): 217–222. doi:10.1016/j.jep.2006.05.004.

46. Kang, B.Y., S.W. Chung, S.H. Kim, S.Y. Ryu, and T.S. Kim. 2000. Inhibition of interleukin-12 and interferon-gamma production in immune cells by tanshinones from Salvia miltiorrhiza. *Immunopharmacology* 49 (3): 355–361.

47. Galis, Z.S., and J.J. Khatri. 2002. Matrix metalloproteinases in vascular remodeling and atherogenesis: The good, the bad, and the ugly. *Circulation Research* 90 (3): 251–262.

48. Pasterkamp, G., A.H. Schoneveld, D.J. Hijnen, D.P. de Kleijn, H. Teepen, A.C. van der Wal, and C. Borst. 2000. Atherosclerotic arterial remodeling and the localization of macrophages and matrix metalloproteases 1, 2 and 9 in the human coronary artery. *Atherosclerosis* 150 (2): 245–253.

49. Fang, Z.Y., R. Lin, B.X. Yuan, Y. Liu, and H. Zhang. 2007. Tanshinone IIA inhibits atherosclerotic plaque formation by down-regulating MMP-2 and MMP-9 expression in rabbits fed a high-fat diet. *Life Sciences* 81 (17–18): 1339–1345. doi:10.1016/j.lfs.2007.08.043.

50. Fang, J., S.W. Xu, P. Wang, F.T. Tang, S.G. Zhou, J. Gao, J.W. Chen, H.Q. Huang, and P.Q. Liu. 2010. Tanshinone II-A attenuates cardiac fibrosis and modulates collagen metabolism in rats with renovascular hypertension. *Phytomedicine : international journal of phytotherapy and phytopharmacology* 18 (1): 58–64. doi:10.1016/j.phymed.2010.06.002.

51. Taganov, K.D., M.P. Boldin, K.J. Chang, and D. Baltimore. 2006. NF-kappaB-dependent induction of microRNA miR-146, an inhibitor targeted to signaling proteins of innate immune responses. *Proceedings of the National Academy of Sciences of the United States of America* 103 (33): 12481–12486. doi:10.1073/pnas.0605298103.

52. Cheng, H.S., N. Sivachandran, A. Lau, E. Boudreau, J.L. Zhao, D. Baltimore, P. Delgado-Olguin, M.I. Cybulsky, and J.E. Fish. 2013. MicroRNA-146 represses endothelial activation by inhibiting pro-inflammatory pathways. *EMBO Molecular Medicine* 5 (7): 1017–1034. doi:10.1002/emmm.201202318.

53. Li, X., D. Kong, H. Chen, S. Liu, H. Hu, T. Wu, J. Wang, W. Chen, Y. Ning, Y. Li, and Z. Lu. 2016. miR-155 acts as an anti-inflammatory factor in atherosclerosis-associated foam cell formation by repressing calcium-regulated heat stable protein 1. *Scientific reports* 6: 21789. doi:10.1038/srep21789.

54. O'Connell, R.M., K.D. Taganov, M.P. Boldin, G. Cheng, and D. Baltimore. 2007. MicroRNA-155 is induced during the macrophage inflammatory response. *Proceedings of the National Academy of Sciences of the United States of America* 104 (5): 1604–1609. doi:10.1073/pnas.0610731104.

55. Gao, Y., J. Peng, Z. Ren, N.Y. He, Q. Li, X.S. Zhao, M.M. Wang, H.Y. Wen, Z.H. Tang, Z.S. Jiang, G.X. Wang, and L.S. Liu. 2016. Functional regulatory roles of microRNAs in atherosclerosis. *Clinica chimica acta; international journal of clinical chemistry* 460: 164–171. doi:10.1016/j.cca.2016.06.044.